



The effect of OH radicals on Cr–I spectral lines emitted by DC glow discharges

P. Mezei ^{a,*}, T. Cserfalvi ^{b,2}, P. Hartmann ^{a,1}, L. Bencs ^{a,1}

^a Research Institute for Solid State Physics and Optics of the Hungarian Academy for Sciences, H-1525 Budapest, 114. P.O.B. 49., Hungary

^b Aqua-Concorde Water Analysis R&D LLC, H-1545 Budapest, Bosnyák u. 11, Hungary

ARTICLE INFO

Article history:

Received 21 September 2009

Accepted 13 February 2010

Available online 20 February 2010

Keywords:

Electrolyte cathode

Atmospheric glow discharge

Atomic emission spectroscopy

ABSTRACT

The intensity distribution of the Cr–I 428.97 nm resonant and 520.60 nm non-resonant lines was studied as a function of the distance from the anode in a low pressure DC-GD fitted with a Cr metal cathode and operated in various gas atmospheres, including helium ($P=4$ mbar), ambient air and water vapor ($P=0.8$ mbar). In the helium and ambient air atmospheres, the intensity peaks occurred in the near cathode region (cathode glow) in accordance with the literature. When operated in water vapor, however, the Cr–I 428.97 nm resonant line disappeared, whereas the intensity of the non-resonant 520.60 nm line was enhanced. This result may be attributed to resonant energy transfer collisions taking place between OH radicals excited to the first vibrational level and Cr^I₄₂₈ atoms excited to the z^7P^0 upper level of the 428.97 nm transition. The similar gas phase composition encountered with a DC electrolyte cathode atmospheric pressure glow discharge (ELCAD) and the Cr metal cathode GD operating under a low pressure of water vapor suggests that the zero intensity of the Cr resonance lines (428.97 nm, 360.53 nm) produced in the ELCAD may be attributed to similar energy transfer processes. Our results show that the intensity of the Cr–I 520.60 nm line can be used for analytical purposes in the ELCAD.

© 2010 Elsevier B.V. All rights reserved.

1. Introduction

The electrolyte cathode atmospheric glow discharge (ELCAD) was first described as a new optical emission source for monitoring the metal content of solutions [1]. For this purpose, the atomic resonant spectral lines emitted by the direct current (DC) ELCAD have generally been used and several heavy metals (e.g., Zn, Cu, Cd, Ni and Pb) can be determined by ELCAD spectrometry. However, several important toxic elements (e.g., Cr and Hg) cannot yet be detected [1–3]. It is well known that contamination of wastewaters by Cr is a serious environmental problem in industrialized regions. Because of this concern, the development of an effective method for monitoring the concentration of Cr pollution in natural and waste waters is a principal research goal with ELCAD. In accordance with a model for plasma sputtering in an electrolyte solution that well describes characteristics for a wide range of elements, Cr has one of the highest sputtering rates [1,3]. The excitation energies of the most intense resonant Cr–I lines widely used in arc, spark and inductively coupled plasma (ICP) sources lie in the range of 2.89–

3.46 eV. Therefore, it is expected that Cr–I lines emitted by the ELCAD should be easily adopted for monitoring the Cr content of aqueous solutions. Unfortunately, spectra emitted from the ELCAD plasma do not contain such resonant Cr–I lines; resonant ultraviolet ($\lambda=357.87$ – 360.53 nm) lines of Cr–I are completely missing and the visible lines ($\lambda=425.43$ – 428.97 nm) are very faint [1–3]. However, a non-resonant transition system near 520 nm appears to be suitable for practical analytical purposes.

To understand these observations, it is necessary to study the effect of different gas atmospheres on Cr–I line intensities. Since the ELCAD operates in an environment saturated with water vapor [1,4] due to the sputtering of the solution cathode, very little of the outer (e.g., atmospheric) gases enveloping the plasma can diffuse into this region. Consequently, the intensity of the atomic lines of metals are found to be independent of the nature of the applied (outer) gas (Ar, N₂) atmosphere [4,5].

Considering the above, it is evident that the plasma atmosphere can be changed only if the solution cathode is replaced by a metal cathode (i.e., in our case by a Cr metal cathode). In such a classical arrangement of a DC-GD, the intensity of the atomic Cr lines ($\lambda=428.97$, 520.60 nm) can be easily studied in different gas atmospheres.

At the atmospheric pressure, the emitting cross-section of a Cr metal cathode DC-GD was quite narrow, i.e., similar to a filament [6–8]. Furthermore, the low average electron energy and low rate of cathode sputtering at high pressure significantly decreased the emission intensity of atomic metal lines.

* Corresponding author: Research Institute for Solid State Physics and Optics of the Hungarian Academy of Sciences, H-1525 Budapest, POB 49, Hungary. Tel.: +36 1 392 22 22/1692; fax: +36 1 392 22 15.

E-mail address: mezeipal@szfki.hu (P. Mezei).

¹ www.szfki.hu.

² www.aqua-concorde.hu.

To obtain higher intensities, measurements were thus conducted in low pressure DC-GDs fitted with a Cr-cathode operating in He ($P=4$ mbar), ambient air and H_2O vapor ($P=0.8$ mbar).

2. Experimental

A low pressure (4 mbar for He, 0.8 mbar for ambient air and H_2O vapor) discharge was produced in a closed chamber with a side quartz window for the optical measurements. At the bottom of the chamber a Cr metal plate served as the cathode and a stainless steel anode plate was placed 50 mm above it. At the applied low pressure, a high rate of cathode sputtering, hence a relatively high intensity of the Cr-I lines could be obtained. As well, with this geometry (large electrode distance) the different parts of the glow discharge could be well distinguished. A flowing gas system was applied within the chamber with a gas flow rate of 2.5 cm³/min. The discharge current was 4 mA.

To study the intensity distribution of the spectral lines, the discharge was vertically scanned by means of a glass optical fiber connected to the 0.3 mm wide entrance slit of a ZEISS PGS 2 monochromator. The glass fiber optic cable was moved by an electric stepper motor along the vertical axis of the discharge in 0.5 mm steps while the intensities were detected by a photomultiplier tube (Pacific Photometrics Instruments, Type 62/3A14). A PC controlled the stepper motor and evaluated the measured intensity data yielding intensity distributions as a function of distance from the anode. At every measurement point, the signal of the photomultiplier was averaged over a time period of 4 s by means of a digital storage oscilloscope.

The intensity distributions of the resonant Cr-I 428.97 nm line and the non-resonant 520.60 nm line as a function of the distance from the anode were recorded. Experiments were performed in helium, ambient air and H_2O vapor atmospheres, with the latter being produced by means of a self-controlling evaporation system shown in Fig. 1. In order to change the atmosphere in the $V \approx 1000$ cm³ discharge vessel, several intermittent evacuations and fillings were applied to achieve >99% of the desired final composition (1 min flushing with ambient air \Rightarrow 2.5 cm³ air at 1 bar \Rightarrow 3130 cm³ at 0.8 mbar; 10 min flushing with water vapor \Rightarrow 25 cm³ vapor at 200 mbar \Rightarrow 3000 cm³ at 0.8 mbar).

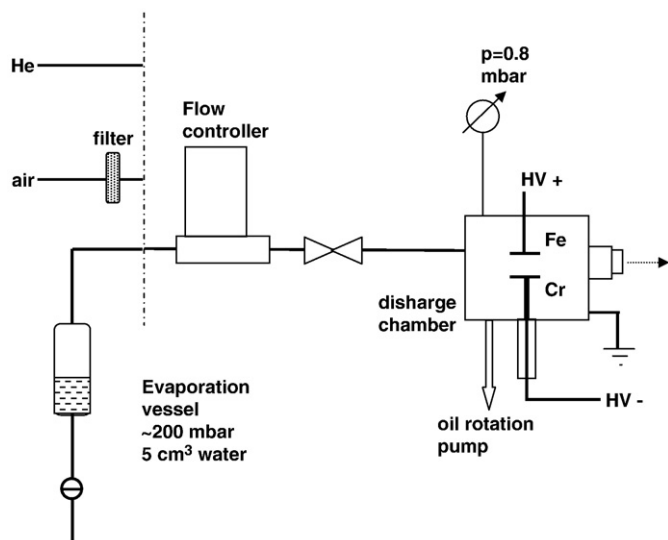


Fig. 1. Schematic of the atmosphere control system.

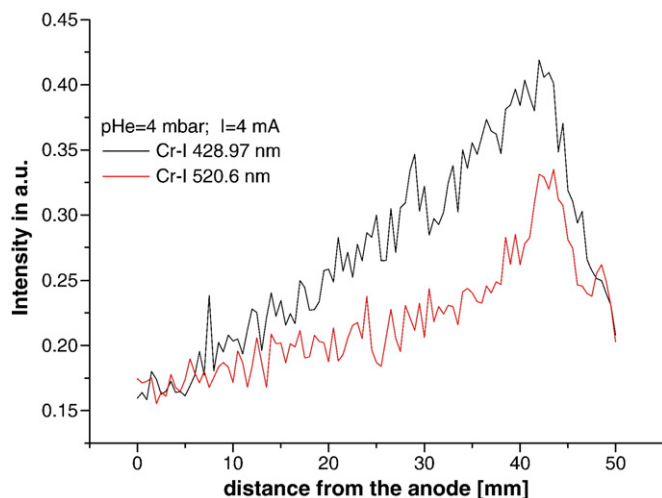


Fig. 2. Intensity distribution of the Cr-I 428.97 nm line as a function of the distance from the anode in a helium atmosphere.

3. Results

3.1. Measurements in He atmosphere

In a helium atmosphere, the intensities of the Cr-I 428.97 nm and 520.60 nm lines increased with distance from the anode; a maximum occurring near the cathode region, as shown in Fig. 2. These intensity distributions are in accordance with that obtained in a low pressure GD [9–11] and the relative magnitude of the intensities corresponds to the excitation energy of the transition.

3.2. Observations in air and water vapor

In ambient air, the Cr-I 428.97 nm line shows classical behavior, illustrated in Fig. 3. Two peaks occur, a wide, slightly lower peak followed by a second, narrow one appearing in front of the cathode. This later can be considered as the cathode glow occurring at sufficient low pressure conditions. This behavior also agrees with results obtained in low pressure DC-GDs [9–11]. However, in the presence of water vapor, the intensities were completely suppressed over the whole discharge volume.

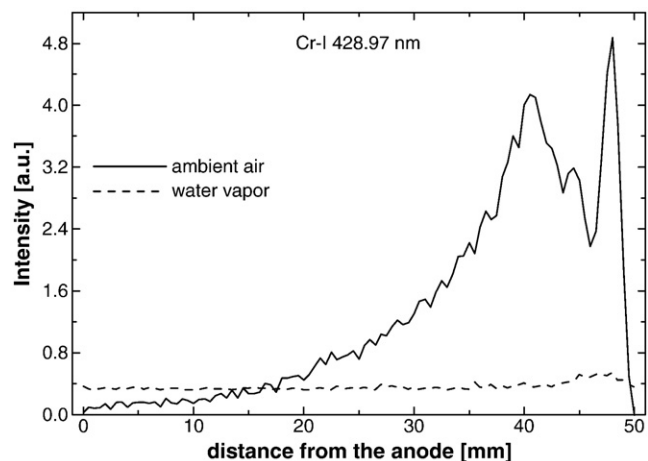


Fig. 3. Intensity distribution of the Cr-I 428.97 nm line as a function of distance from the anode in ambient air and H_2O vapor discharges.

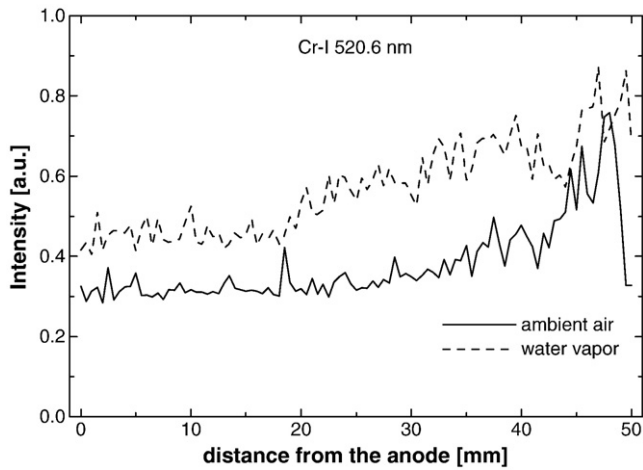


Fig. 4. Intensity distribution of the Cr-I 520.60 nm line as a function of the distance from the anode in ambient air and H₂O vapor discharges.

The intensity distribution of the non-resonant Cr-I 520.60 nm line also exhibits classical behavior in the ambient air atmosphere, similar to that generated in He gas. However, in the presence of water vapor, its intensity increased over the entire discharge volume compared with that observed in air and He gases (Fig. 4).

4. Discussions

The resonant Cr-I 428.97 nm line corresponds to a $z^7P^0 \rightarrow a^7S$, the non-resonant 520.60 nm line does to a $z^5P^0 \rightarrow a^5S$ one. The energy of z^7P^0 level is 2.89 eV and that of z^5P^0 level is 3.32 eV [12]. The energy difference Δ between the z^7P^0 and z^5P^0 upper levels is very small:

$$\Delta = E(z^5P^0) - E(z^7P^0) = E_{520} - E_{428} = 0.43 \text{ eV}. \quad (1)$$

In He gas, the intensity distributions of the Cr-I 428.97 nm and the 520.60 nm lines were found to be similar.

Considering relation (1) and that the energy of excited He levels are significantly higher than either of these two atomic Cr transitions, the resulting similar intensity distributions may be attributed to the following processes: the cathode sputtering produce the neutral metal atoms which are excited by electron impact. This is in accordance with observations in classical low pressure DC-GDs [9–11].

In the ambient air atmosphere at a pressure of 0.8 mbar, the Cr-I 428.97 nm and 520.60 nm lines can be detected. Their similar behaviors are also in accordance with classical low pressure DC-GD operation [9–11].

In the intensity distribution of the Cr-I 428.97 nm line, the cathode glow appeared in the front of the cathode. This is a well-known and thoroughly studied phenomenon in the DC-GDs operating at the sufficient low pressures and corresponding high electrode distance. In this case, a high number of fast ions and neutral particles are present in the near cathode region. If their energy is enough, they are able to excite via collisions the corresponding atomic transitions [9–11]. Since the effects observed in the H₂O vapor are relevant for us, we are not dealing with the more detailed investigation of this phenomenon.

In the other part of the discharge, the measured intensity distribution indicates that the neutral Cr atoms produced by the cathode sputtering are excited by electron impact.

In the presence of water vapor, the intensity of the Cr-I 428.97 nm was suppressed over the entire discharge volume, while that of the Cr-I 520.60 nm was enhanced throughout the whole discharge volume.

If we suppose that both z^7P^0 and z^5P^0 upper levels are excited only by electron impact, we obtain the similar rate equation [13] for both levels. Under steady state conditions:

$$\frac{dN_{Cr}^*}{dt} = n_e N_{Cr}^0 \langle \sigma_{el} v_e \rangle - AN_{Cr}^* = 0 \quad (2)$$

where n_e is the electron density, N_{Cr}^0 is the density of ground state Cr atoms, σ_{el} is the cross-section for electron impact excitation, v_{el} is the velocity of electrons, N_{Cr}^* is the Cr-atom density in the upper level, and A is the transition probability. Expressing N_{Cr}^* from relation (2), the emitted intensity is:

$$I = N_{Cr}^* Ah\nu = h\nu \cdot n_e N_{Cr}^0 \langle \sigma_{el} v_e \rangle. \quad (3)$$

For Cr-I 428.97 nm line, the emitted photon energy is $h\nu = 2.89$ eV, in the case of the Cr-I 520.60 nm line it is $h\nu = 2.38$ eV, the difference between them is very small (0.51 eV), hence $h\nu$ can be considered about the same for both cases. N_{Cr}^0 and n_e are the same for both upper levels. The values of $\langle \sigma_{el} v_e \rangle$ can be considered to be the same for both upper levels, since the electron velocity is the same and the σ_{el} cross-section of electron impact excitation is nearly the same for both transitions because of relation (1). In this way, we obtain about the same intensity for both Cr-I lines.

But this result does not agree with the experiments. The correct interpretation of experimental observations requires to take into account another process besides the electron impact excitation, which simultaneously depopulates the z^7P^0 level and populates the z^5P^0 one.

A DC-GD operating in H₂O vapor (ELCAD) was also investigated in detail. The ELCAD plasma operates in a saturated water vapor at atmospheric pressure, in which H₂O⁺ molecular ions are the positive ions [14,15]. In the cathode dark space, the main loss of these molecular ions occurs via dissociative recombination, producing H and OH species [14,15]:



The rate of reaction (4) is [16,17]:

$$r \approx (kT_e)^{-1/2} \approx \sqrt{p} \quad (5)$$

where p is the pressure, k is the Boltzmann-constant and T_e is the electron temperature.

The intensity maximum of the emitted metal atomic spectral lines appeared in the negative glow region of the ELCAD plasma. In this region, the gas and electron temperatures were found to be $T_e \approx T_{gas} \approx 7000$ K [1,2]. For such a high temperature, the rate coefficient of the dissociative recombination ($k_{d,r}$) [15] is:

$$k_{d,r} \approx 4.4 \times 10^{-8} \text{ cm}^3 \text{ s}^{-1} \quad (6)$$

Furthermore, the thermal dissociation of water was thermodynamically modeled. The equilibrium composition was calculated by using the free enthalpy minimization. It was found, that above $T \approx 4500$ K all the H₂O molecules dissociate to OH and H [18].

The thermal dissociation (the thermolysis) of water molecule is given by the following reaction:



At the temperature of $T_e \approx T_{gas} \approx 7000$ K, the rate coefficient of reaction (7) (k_{th}) is [19]:

$$k_{th} \approx 3.1 \times 10^{-9} \text{ cm}^3 \text{ s}^{-1}. \quad (8)$$

The high value of the rate coefficients $k_{d,r}$ in Eq. (5) and k_{th} in Eq. (8) indicates that, the reactions (4) and (7) produce a very high number of

OH radicals in the ELCAD plasma. This is supported by the very high intensity of OH bands measured in the ELCAD emission spectrum [1,2,14,20]. Thus, the H_2O^+ molecular ions, OH radicals, and the H atoms are the dominant, stable species in the ELCAD plasma operating in a saturated H_2O vapor. Other species, such as Cr atoms, are generated by cathode sputtering [1]. Since hydrogen is a volatile gas, it rapidly escapes the plasma discharge volume.

At low pressures, the gas temperature T_{gas} ($\sim 10^2$ K, or less) and the density of H_2O molecule are low, while kT_e average electron energy is high (~ 6 – 10 eV) [9–11]. Therefore, the rate of reactions (4) and (7) significantly decrease. But the H_2O molecules can be split by electron collisions also:



The threshold energy of this reaction is 5.1 eV [21–23]. In a low pressure DC-GD, the reaction (9) can produce a high number of OH radical due to the high average electron energy. The rate coefficient of reaction (9) is given only in the case of $T_{gas} = 425$ K [23]:

$$k_{el} \approx 3.57 \times 10^{-10} \text{ cm}^3 \text{ s}^{-1}. \quad (10)$$

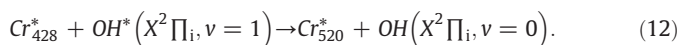
Furthermore, the H_2O^+ molecular ions are the positive ions in a low pressure water vapor also [15]. Therefore, it may be assumed that a DC-GD fitted with a metal cathode of Cr operating in H_2O vapor at a pressure of 0.8 mbar contains the same dominant species, but at a lower density due to the lower pressure. Additionally, the Cr atoms generated by cathode sputtering are also firstly excited by electron impact [9–11].

Since the excited atomic hydrogen energy levels (10.2–13.6 eV) are much higher than those of the atomic Cr transitions (2.89–3.46 eV) [12], the H atoms exert no influence on the intensity of the Cr–I lines and they quickly leave the plasma due to their mobility.

The high number of OH radicals appearing in a DC-GD operating in a low pressure of H_2O vapor can be excited by electron impact to various vibrational states. It is significant that the energy of the OH radical excited to its first vibrational level in the $X^2\Pi_i$ electronic ground state is [24–31]:

$$G(v=1) = 3569.59 \text{ cm}^{-1} = 0.44 \text{ eV}. \quad (11)$$

This $G(v=1)$ value is in a close coincidence (within 0.01 eV) with the $\Delta = 0.43$ eV energy difference between z^7P^0 and z^5P^0 upper levels of Cr–I given by relation (1). Considering this close energy coincidence, the occurrence of resonant energy transfer (RET) collisions can be expected between the Cr atoms excited to the z^7P^0 upper level of the 428.973 nm transition (Cr_{428}^*) and the OH radicals excited to their first vibrational state ($OH^*(X^2\Pi_i, v=1)$), i.e.,



The RET collisions (relation (12)) produce excited state Cr atoms in the z^5P^0 upper level of the 520.6 nm transition (Cr_{520}^*) and hydroxyl radicals in their ground state ($OH(X^2\Pi_i, v=0)$). As a result of the close energy coincidence mentioned above (0.01 eV), the cross-section of this RET collision (σ_{RET}) is orders of magnitude higher than that for electron impact excitation (σ_{el}) [13]:

$$\sigma_{RET} \approx 10^{-14} \text{ cm}^2 \gg \sigma_{el} \approx 10^{-18} \text{ cm}^2. \quad (13)$$

This implies that electron impact excitation populates the z^7P^0 upper level of the Cr–I 428.9 nm transition, but RET collisions (relation (12)) are able to convert all Cr atoms from this z^7P^0 upper level to the z^5P^0 upper level of the Cr–I 520.60 nm transition, as illustrated in Fig. 5. Thus, the intensity of the Cr–I 428.97 nm line significantly decreases, i.e. it becomes practically zero, whereas the intensity of the Cr–I 520.60 nm line is enhanced.

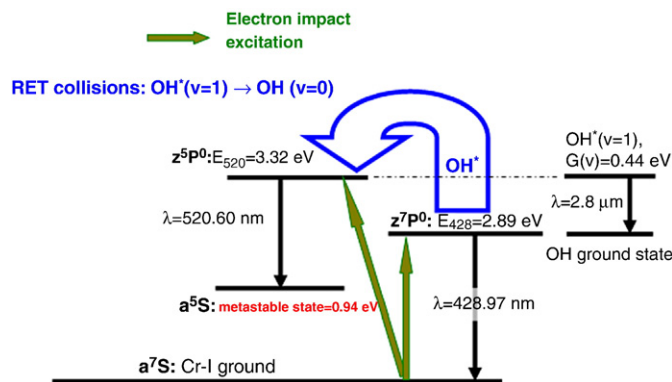


Fig. 5. Excitation scheme for the z^7P^0 upper level of the resonant Cr–I 428.97 nm and the z^5P^0 upper level of the non-resonant Cr–I 520.60 nm transitions.

This discussion correspond to a DC-GD fitted with a Cr metal cathode operating in a low pressure of water vapor. On the basis mentioned above, there is a similarity between the gas phase of the Cr metal cathode discharge operating in a low pressure of H_2O vapor and the ELCAD. Both DC-GDs are operating in the same H_2O vapor containing the same dominant species, including H_2O^+ molecular ions, OH radicals and H atoms. In both H_2O plasmas, the neutral metal atoms are generated by cathode sputtering [1,4,9–11]. In general, these neutral metal atoms are firstly excited by electron impact. These two gas phases differ from each other in their average electron energy, the rate of cathode sputtering and hence their emitted atomic Cr line intensities. On the basis of this, as a first approximation, it can be assumed that the dominant processes determining the occurrence of the atomic Cr lines are very similar in the gas phase of both discharges. In this way, the very faint intensity of the atomic Cr 425.43–428.97 nm lines measured in the ELCAD plasma can also be attributed to similar resonant energy transfer collisions (reaction (12)) between the Cr atoms excited to the z^7P^0 upper level of the 428.97 nm transition (Cr_{428}^*) and hydroxyl radicals excited to their first vibrational level ($OH^*(X^2\Pi_i, v=1)$).

The similarity of both gas phases, the fact that the OH radical has a ninth vibrational state in its $X^2\Pi_i$ electronic ground state [32–36] and its energy is very close to the y^7P^0 upper level energy of the Cr–I 360.53 nm transition suggests that, the practically zero intensity of the ultraviolet resonant Cr–I 360.53 nm line emitted by the ELCAD can be studied by invoking similar RET collisions.

The $G(v=9)$ energy of the OH radical excited to its ninth vibrational state $OH^*(v=9)$ in the $X^2\Pi_i$ electronic ground state can be calculated assuming an anharmonic oscillator approximation by means of the relation [24,25,30]:

$$G(v) = \omega_e \left(v + \frac{1}{2} \right) - \omega_e x_e \left(v + \frac{1}{2} \right)^2 + \omega_e y_e \left(v + \frac{1}{2} \right)^3 - \omega_e z_e \left(v + \frac{1}{2} \right)^4 + \dots \quad (14)$$

In this case, $\omega = \nu/c$, where ν is the vibrational frequency of the anharmonic oscillator and c is the velocity of light. The parameters x_e , y_e and z_e are proportional to the amplitude of the oscillation. Values of $\omega_e x_e$, $\omega_e y_e$, and $\omega_e z_e$ can be found in the literature [24,25,29,30]; thus the value of $G(v=9)$ can be calculated from Eq. (14) (Table 1) as:

$$G(v=9) \approx 3.46 \text{ eV}. \quad (15)$$

Table 1
The calculated $G(v)$ vibrational energies of OH ($X^2\Pi_i, v=0$ – 10) in eV units [24,25,29,30].

| v | V=1 | V=2 | V=3 | V=4 | V=5 | V=6 | V=7 | V=8 | V=9 | V=10 |
|--------|------|------|------|------|------|------|------|------|------|------|
| $G(v)$ | 0.44 | 1.09 | 1.50 | 1.88 | 2.24 | 2.58 | 2.90 | 3.20 | 3.46 | 3.74 |

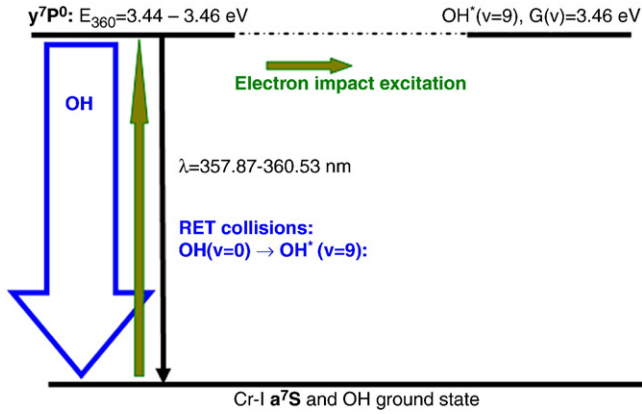
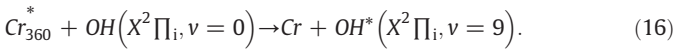


Fig. 6. Excitation scheme of the y^7P^0 upper level of the resonant Cr-I 360.53 nm transition.

Fig. 6 shows that the y^7P^0 upper level energy of the Cr-I 360.53 nm transition is 3.44 eV, which differs from $G(v=9) \approx 3.46$ eV by only 0.02 eV. Because of this close energy coincidence, we can assume that RET collisions occur between the ground state OH radicals and the Cr atoms excited by electron impact to the y^7P^0 upper level of the 360.53 nm transition Cr_{360}^* :



The RET collisions described above (reaction (16)) produce Cr atoms in the ground state (Cr) and hydroxyl radicals excited to their ninth vibrational state $OH^*(X^2\Pi_i, v=9)$. The cross-section of this RET collision is also high ($\sigma_{RET} \approx 10^{-14} \text{ cm}^2$) due to the close energy level coincidence [13]. Therefore, electron impact excitation populates the y^7P^0 upper level of the Cr-I 360.53 nm transition but RET collisions described by reaction (16) are able to convert all Cr atoms from this level to their ground state, as illustrated schematically by Fig. 7. Thus the intensity of the Cr I 360.53 nm line becomes practically zero.

4.1. Estimations for ELCAD

The interpretations relating to the ELCAD can be supported by the simple estimations. To present the dominant effect, it is enough to consider only the order of magnitude of the corresponding data.

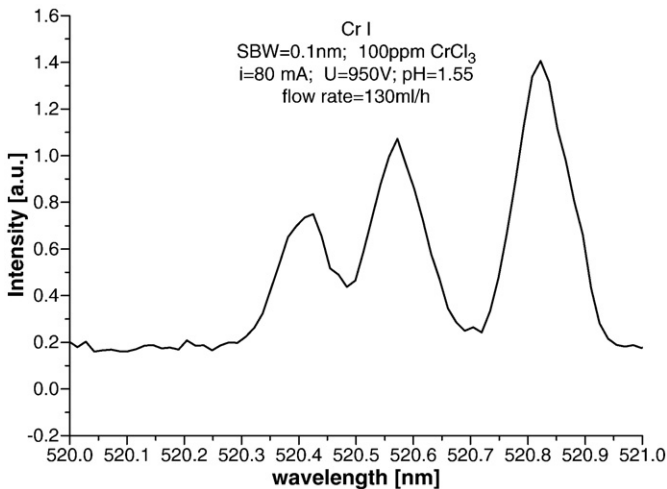


Fig. 7. Intensity of the non-resonant Cr-I 520.45–520.84 nm lines emitted by the ELCAD plasma. Cr concentration: 100 $\mu\text{g/ml}$; discharge voltage: 950 V; current: 80 mA; the solution pH: 1.55, adjusted with HCl.

Under steady state conditions, on the basis of the processes shown by Fig. 5, the Cr atom density in the z^7P^0 upper level of the 428.97 nm transition can be calculated by the following rate equation [13]:

$$\frac{dN_{Cr,428}^*}{dt} = n_e N_{Cr}^0 \langle \sigma_{el} v_e \rangle - A_{428} N_{Cr,428}^* - N_{Cr,428}^* N_{OH}^* \langle \sigma_{RET} v_{OH} \rangle = 0 \quad (17)$$

where n_e is the electron density, N_{Cr}^0 is the density of ground state Cr atoms, σ_{el} is the cross-section for electron impact excitation, v_{el} is the velocity of electrons, $N_{Cr,428}^*$ is the Cr atom density in the z^7P^0 upper level, A_{428} is the transition probability, N_{OH}^* is the density of $OH^*(X^2\Pi_i, v=1)$ (OH excited to the first vibrational state) and v_{OH} is the average velocity of the OH radicals.

On the right side of Eq. (17), the first term describes the electron impact excitation of the upper level, the second indicates the spontaneous emission from this upper level and the third accounts for RET collisions with $OH^*(X^2\Pi_i, v=1)$ radicals.

The $\langle \sigma_{el} v_e \rangle$ and $\langle \sigma_{RET} v_{OH} \rangle$ are integrals which include the product of the corresponding cross-section as a function of energy $\sigma(E)$ and the velocity (or energy) distribution function $v(E)$.

The Cr atom density in the z^7P^0 upper level of the 428.97 nm transition can be expressed from relation (17):

$$N_{Cr,428}^* = \frac{n_e N_{Cr}^0 \langle \sigma_{el} v_e \rangle}{A_{428} + N_{OH}^* \langle \sigma_{RET} v_{OH} \rangle}. \quad (18)$$

In H_2O vapor, the correct form of $\sigma(E)$ and $v(E)$ are unknown, therefore, the values of the $\langle \sigma_{el} v_e \rangle$ and $\langle \sigma_{RET} v_{OH} \rangle$ integrals can only be estimated. As a first approximation, we can assume that $\langle \sigma v \rangle \sim \sigma \cdot v$. Hence, these values can be considered to be correct only within an order of magnitude.

The density of H_2O molecules can be calculated from the ideal gas law [16]:

$$N_{H_2O} = \frac{3.3 \cdot 10^{16} \cdot p[\text{torr}] \cdot 293[\text{K}]}{T_{\text{gas}}}. \quad (19)$$

The intensity peaks of atomic metal lines appear in the negative glow. In this region of the ELCAD plasma operating at atmospheric pressure ($P=760$ torr), the electron T_e and the gas temperature T_{gas} were found to be [2]:

$$T_e \approx T_{\text{gas}} \approx 7000 \text{ K}. \quad (20)$$

Substituting these values into relation (19), we obtain the density of H_2O molecules:

$$N_{\text{water}} \approx 10^{18} \text{ cm}^{-3} \quad (21)$$

however, at such high temperatures ($T_{el} \approx T_G \approx 7000$ K), all H_2O molecules would be dissociated through thermolysis[18], thus:

$$N_{\text{water}} \approx N_{OH}^0 \approx 10^{18} \text{ cm}^{-3}. \quad (22)$$

The density of excited $OH^*(v=1)$ radicals (N_{OH}^*) can be estimated by means of the Boltzmann-distribution:

$$N_{OH}^* = N_{OH}^0 \cdot \exp\left(-\frac{E = G(v=1)}{kT_e}\right). \quad (23)$$

Using relations (11), (20) and (21), we obtain:

$$N_{OH}^* \approx 5 \cdot 10^{17} \text{ cm}^{-3}. \quad (24)$$

Applying relation (20) and $m_{\text{OH}} \approx 7 \times 10^{-26}$ kg, the average velocity of OH radicals can be estimated:

$$v_{\text{OH}} = \sqrt{\frac{3kT_{\text{gas}}}{m_{\text{OH}}}} \approx 2 \cdot 10^5 \text{ cm} \cdot \text{s}^{-1}. \quad (25)$$

In a similar way, we can obtain the average velocity of electrons:

$$v_{\text{el}} = \sqrt{\frac{3kT_e}{m_{\text{el}}}} \approx 6 \cdot 10^7 \text{ cm} \cdot \text{s}^{-1}. \quad (26)$$

The electron density is given by [37]:

$$n_{\text{el}} \approx 2 \cdot 10^{13} \text{ cm}^{-3}. \quad (27)$$

The transition probability is [12]:

$$A_{428} = 3 \cdot 10^7 \text{ s}^{-1}. \quad (28)$$

Substituting relations (13), (24), (25), (26), (27) and (28) into Eq. (18), we obtain the Cr atom density in the upper level of the 428.97 nm transition:

$$\frac{N_{\text{Cr},428}^*}{N_{\text{Cr}}^0} \approx 10^{-6}. \quad (29)$$

This result indicates that the Cr atom density in the z^7P^0 upper level is 10^{-6} times lower than that of the a^7S ground state. Hence, the upper level density is practically zero, i.e., the RET collisions effectively convert nearly all Cr atoms from the upper level of the 428.97 nm transition. If the ratio of the Cr-atom density on the z^7P^0 upper level and a^7S ground state is calculated only by means of the Boltzmann-distribution, the result is 8.3×10^{-3} . This is higher with three orders of magnitude than Eq. (29) demonstrating that the RET collisions can indeed effectively convert all Cr atoms from the z^7P^0 upper level to the z^5P^0 one.

The Cr-I $z^7P^0 \rightarrow a^7S$ transition is a series containing $\lambda = 425.43$ nm, $\lambda = 427.48$ nm and $\lambda = 428.97$ nm lines. Their upper level energy is in order of 2.91 eV, 2.90 eV and 2.89 eV. Hence the energy difference Δ between them and $G(v=1) = 0.44$ eV vibrational energy of $\text{OH}^*(X^2\Pi_i, v=1)$ are in order of 0.03 eV, 0.02 eV and 0.01 eV. The highest value of $\Delta = 0.03$ eV obtained with the upper level energy of 425.43 nm transition. In this case, the cross-section of RET collisions is $\sigma_{\text{RET}} \approx 10^{-15} \text{ cm}^2$ [13]. Using this data in relation (18), the ratio of Cr-atom density of z^7P^0 and a^7S levels is:

$$\frac{N_{\text{Cr},428}^*}{N_{\text{Cr}}^0} \approx 10^{-5}. \quad (30)$$

From the Boltzmann-distribution (corresponds to the electron impact excitation only) is obtained:

$$\frac{N_{\text{Cr},428}^*}{N_{\text{Cr}}^0} \approx 10^{-3}. \quad (31)$$

The value of Eq. (30) is lower with two orders of magnitude than that of Eq. (31) indicating that the RET collisions determine the population of the upper level of 425.43 nm transition. In the case of 427.48 nm and 428.97 nm transitions, the values of Δ are lower than 0.03 eV resulting in higher σ_{RET} values. Therefore, the RET collisions determine the upper level population of these two transitions also.

The density of Cr atoms in the y^7P^0 upper level of the 360.53 nm transition can be estimated also by using the relations presented above.

The relation corresponding to Eq. (18) is:

$$N_{\text{Cr},360}^* = \frac{n_e \cdot N_{\text{Cr}}^0 \cdot \langle \sigma_e \cdot v_e \rangle}{A_{360} + N_{\text{OH}}^0 \cdot \langle \sigma_{\text{RET}} \cdot v_{\text{OH}} \rangle}. \quad (32)$$

In this case, the transition probability is [12]:

$$A_{360} \approx 3 \cdot 10^7 \text{ s}^{-1}. \quad (33)$$

Substituting Eqs. (13), (22), (25)–(27) and (33) into Eq. (32), we obtain:

$$N_{\text{Cr},360}^* \sim N_{\text{Cr}}^0 \cdot 3 \cdot 10^{-7} \text{ cm}^{-3}. \quad (34)$$

Eq. (34) indicates that the density of Cr atoms in the y^7P^0 upper level is 10^{-7} times lower than that of the a^7S ground state. Hence, the y^7P^0 upper level density is practically zero, i.e., RET collisions effectively convert nearly all Cr atoms from the y^7P^0 upper level of the 360.53 nm transition to the a^7S ground state. The ratio of Cr-atom density on y^7P^0 upper level and the a^7S ground state determined only by means of the Boltzmann-distribution is 3.4×10^{-3} . This is higher with four orders of magnitude than Eq. (34) supporting that the RET collisions can indeed effectively convert all Cr atoms from the y^7P^0 upper level to the a^7S ground state.

But the Cr-I $y^7P^0 \rightarrow a^7S$ transition is also a series containing the $\lambda = 357.87$ nm, $\lambda = 359.35$ nm and $\lambda = 360.53$ nm lines. Their upper level energy is in order of 3.46 eV, 3.45 eV and 3.44 eV. The vibrational energy of $\text{OH}^*(X^2\Pi_i, v=9)$ is $G(v=9) = 3.46$ eV. The highest $\Delta = 0.02$ eV energy difference between these Cr-I levels and $\text{OH}^*(X^2\Pi_i, v=9)$ can be obtained ($\Delta = 0.02$ eV), with the upper level energy of 360.53 nm transition. In this case, the cross-section of RET collisions is $\sigma_{\text{RET}} \approx 10^{-15} \text{ cm}^2$ [13], hence the ratio of Cr-atom densities of y^7P^0 and a^7S levels is:

$$\frac{N_{\text{Cr},360}^*}{N_{\text{Cr}}^0} \approx 4.5 \cdot 10^{-5}. \quad (35)$$

Again, from the Boltzmann-distribution gives:

$$\frac{N_{\text{Cr},360}^*}{N_{\text{Cr}}^0} \approx 3.4 \cdot 10^{-3}. \quad (36)$$

The value of Eq. (35) is lower with two orders of magnitude than that of Eq. (36). This comparison indicates, that in this case, the RET collisions determine the upper level population of Cr-I 360.53 nm transition. Because of similar reasons mentioned above, this is valid for the upper level population of the 357.87 nm–360.53 nm transitions also.

The estimations presented above for the case of ELCAD indicate the very high efficiency of RET collisions. This is caused by not only the high value of σ_{RET} due to the close energy coincidence between the corresponding excited atomic Cr and OH levels, but the very high density of OH radicals also produced by reactions (4) and (7). Considering the result reported in Ref. [18], at the temperature of $T_{\text{el}} \approx T_G \approx 7000$ K, all H_2O molecules dissociate to H and OH.

As our results show, in the case of the ELCAD, the intensity of the Cr-I non-resonant lines emitted at 520.45–520.84 nm can be used for the determination of the Cr content of the electrolyte solution. The intensities of these Cr-I non-resonant green lines were measured as a function of the wavelength emitted by the ELCAD plasma. In this case, CrCl_3 was dissolved in the cathode solution to provide a concentration of 100 $\mu\text{g}/\text{mL}$ and the pH was adjusted to 1.55 with HCl. The discharge voltage was 950 V, the current was $I = 80$ mA and a solution flow rate of 130 ml/h was used. The resultant spectra are shown in Fig. 7. Using a flow injection analysis system and measuring the intensity of the Cr I

520.60 nm line emitted by the ELCAD plasma, a LOD of 0.5 µg/ml was attained for detection of Cr.

But in the ELCAD emitted spectrum, the measured intensity of the Cr–I 520.60 nm line was not so high compared with that obtained for Zn–I 213.8 nm and Cd–I 228.8 nm lines. Since the a^5S lower level of the Cr–I 520.60 nm transition is a metastable state, it is plausible to assume as a first, approximation, that the Cr atoms can accumulate on this a^5S lower level. During the lifetime of this metastable state, transitions from this level to the ground state cannot occur. In this manner, the rate of transitions of Cr atoms from here to the ground state can be small, hence the number of Cr atoms available for further excitation can be limited. Of course, this interpretation is only a possible assumption, it is necessary to perform further experiments to support it.

5. Conclusions

The intensity distributions of the Cr–I resonant 428.97 nm and the non-resonant 520.60 nm lines were investigated as a function of distance from the anode in a DC glow discharge fitted with a Cr metal plate as a cathode and operated at pressures of 0.8–4 mbar. Experiments were conducted in helium, ambient air, and in water vapor.

In helium and ambient air atmospheres, the resultant intensity distributions were in accordance with those obtained in such low pressure DC glow discharges, indicating that the intensity of the Cr atomic lines is determined by the rates of cathode sputtering and electron impact excitation. In the water vapor atmosphere, however, the intensity of the Cr–I 428.97 nm resonant line practically disappeared, while that of the Cr–I 520.60 nm line was enhanced, a consequence of RET collisions between excited Cr^+_{428} atoms and the excited $OH^+(v=1)$ radicals. These RET collisions simultaneously depopulate the z^7P^0 upper level of the Cr–I 428.97 nm line and populate the z^5P^0 upper level of the Cr–I 520.60 nm line, resulting in a practically zero intensity of the Cr–I 428.97 nm line and an enhanced intensity of the 520.60 nm line.

Considering that similar gas phases occur with the ELCAD plasma and the Cr metal cathode discharge operating in a low pressure water vapor, it has been shown that the very faint intensity of the atomic Cr–I 428.97 nm line emitted by the ELCAD can be explained by similar RET collisions. On the basis of the similar gas phases for both discharges, the nearly zero intensity of the Cr–I 360.53 nm line obtained in the ELCAD could also be explained by RET collisions between the excited Cr^+_{360} atoms and ground state OH radicals.

The emitted intensity of Cr–I 520.45–520.84 nm lines can be used for analytical purposes with the ELCAD source.

Acknowledgement

This work was supported by the Hungarian Scientific Research Fund (OTKA) under the project number of K 68390.

References

- [1] P. Mezei, T. Cserfalvi, Electrolyte cathode atmospheric glow discharges for direct solution analysis, *Appl. Spectr. Rev.* 42 (2007) 573–603.
- [2] P. Mezei, T. Cserfalvi, L. Csillag, The spatial distribution of the temperatures and the emitted spectrum in the electrolyte cathode atmospheric glow discharge, *J. Phys. D Appl. Phys.* 38 (2005) 2804–2811.
- [3] T. Cserfalvi, P. Mezei, Investigation on the element dependency of sputtering processes in the electrolyte cathode atmospheric discharge, *J. Anal. At. Spectrom.* 20 (2005) 939–944.
- [4] A. Hickling, Electrochemical processes in glow discharge electrolysis at gas-solution interface, in: J.M. Bockris, B.E. Conway (Eds.), *Modern aspects in Electrochemistry* vol. 6, Butterworths, London, 1971.
- [5] Y.S. Park, S.H. Ku, S.H. Hong, H.J. Kim, E.H. Piepmeier, Fundamental studies of electrolyte-as-cathode glow discharge-atomic emission spectroscopy for determination of trace metals in flowing water, *Spectrochim. Acta Part B* 53 (1998) 1167–1179.
- [6] W.A. Gambling, H. Edels, The high pressure glow discharge in air, *Brit. J. Appl. Phys.* 5 (1954) 36–39.
- [7] T.J. Massey, Constricted discharges in the rare gases II. Analysis of the macroscopic properties of the discharges, *J. Appl. Phys.* 36 (1965) 373–380.
- [8] P. Mezei, T. Cserfalvi, M. Jánossy, On the pressure dependence of the positive column cross section in a high-pressure glow discharge, *J. Phys. D Appl. Phys.* 34 (2001) 1914–1918.
- [9] G. Francis, The Glow discharge at low pressure, in: S. Flügge (Ed.), *Encyclopedia of Physics* vol. 22, Spriger, Berlin, 1956, pp. 53–208.
- [10] D. Marić, P. Hartmann, G. Malović, Z. Donkó, Z.L. Petrović, Measurements and modelling of axial emission profile in abnormal glow discharges in argon: heavy-particles processes, *J. Phys. D Appl. Phys.* 36 (2003) 2639–2648.
- [11] K. Rózsa, A. Gallagher, Z. Donkó, Excitation of Ar lines in the cathode region of a dc discharge, *Phys. Rev. E* 52 (1) (1995) 913–918.
- [12] NIST (National Institute of Standard and Technology) *Atomic Spectroscopy Database* <http://physics.nist.gov/phys.ref.data>.
- [13] C.S. Willett, *Introduction to Gas Lasers: Population Inversion Mechanisms*, Pergamon Press, Oxford, 1974.
- [14] P. Mezei, T. Cserfalvi, M. Jánossy, K. Szöcs, H.J. Kim, Similarity laws for glow discharges with cathodes of metal and an electrolyte, *J. Phys. D Appl. Phys.* 31 (1998) 2818–2825.
- [15] T.J. Dolan, Electron and ion collisions with water vapour, *J. Phys. D Appl. Phys.* 26 (1993) 4–8.
- [16] Y.P. Raiser, *Gas Discharge Physics*, Springer, Berlin, 1991.
- [17] H.S.W. Massey, W.B. Gilbody, Recombination, in: H.S.W. Massey, et al., (Eds.), *Electronic and Ionic Impact Phenomena* vol. IV, Clarendon, Oxford, 1974.
- [18] N. Boudesocque, C. Vandesteendam, C. Lafon, C. Girold, Hydrogen production by thermal water splitting using a thermal plasma, in: *Proceedings of the 16th World Hydrogen Energy Conference, WHEC 16*, 13–16 June Lyon, France, 2006.
- [19] NIST Chemical Kinetic Database, <http://kinetics.nist.gov/kinetics>.
- [20] T. Cserfalvi, P. Mezei, Direct solution analysis by glow discharge: electrolyte-cathode discharge spectrometry, *J. Anal. At. Spectrom.* 9 (1994) 345–349.
- [21] S. Medovic, B.R. Locke, Primary chemical reactions in pulsed electrical discharge channels in water, *J. Phys. D Appl. Phys.* 40 (2007) 7734–7746.
- [22] B. Ruscic, A.F. Wagner, L.B. Harding, R.L. Asher, et al., On the enthalpy of formation of hydroxyl radical and gas-phase bond dissociation energies of water and hydroxyl, *J. Phys. Chem. A* 106 (2002) 2727–2747.
- [23] I.A. Soloshenko, V.V. Tsiolko, S.S. Pogulay, et al., Effect of water adding on kinetics of barrier discharge in air, *Plasma Source Sci. Technol.* 18 (2009) 045019 (15pp).
- [24] G.H. Dieke, H.M. Crosswhite, The ultraviolet bands of OH, *J. Quant. Spectrosc. Radiat. Transfer.* 2 (1961) 97–199.
- [25] G. Herzberg, *The spectra and structures of simple free radicals*, An introduction to molecular spectroscopy, Cornell University Press, Ithaca, London, 1971.
- [26] R. Mavrodineanu, H. Boiteux, *L'Analyse Spectrale Quantitative par La Flamme*, Masson et Cie, Paris, 1954.
- [27] V.S. Strel'nitskii, Cosmic masers, *Sov. Phys. Usp.* 17 (4) (1975) 507–527.
- [28] www.cfa.harvard.edu/HITRAN.
- [29] J.R. Bochinski, E.R. Hudson, H.J. Lewandowski, Jun Ye, Cold free-radical molecules in the laboratory frame, *Phys. Rev. A* 70 (2004) 043410 (18pp).
- [30] J. Luque, D.R. Crosley, Transition probabilities in the $A^2\Sigma^+ - X^2\Pi$ electronic system of OH, *J. Chem. Phys.* 109 (2) (1998) 439–448.
- [31] B. Rosen, *Spectroscopic Data relative to Diatomic Molecules*, in *International Tables of Selected Constants* 17, Pergamon Press, Oxford, 1970.
- [32] J.D. Mckinley, J.D. Garvin, M.J. Boudart, Production of excited hydroxyl radicals in the hydrogen atom-ozone reaction, *J. Chem. Phys.* 23 (5) (1955) 784–786.
- [33] D. Garvin, H.P. Broida, H.J. Kostkowski, Chemically induced vibrational excitation: hydroxyl radical emission in the 1–3 micron region by the $H+O_3$ atomic flame, *J. Chem. Phys.* 32 (3) (1960) 880–887.
- [34] P. Colin, P.F. Coheur, M. Kiseleva, A. Vandeale, P.F. Bernath, Spectroscopic constants and term values for the $X^2\Pi_1$ state of $OH(v=0-10)$, *J. Mol. Spectrosc.* 214 (2002) 225–226.
- [35] D.D. Nelson, A. Schiffmann, J. Nesbit, Absolute infrared moments for open shell diatomics for J dependence of transition intensities: application to OH, *J. Chem. Phys.* 90 (1989) 5443–5454.
- [36] A. Goldman, W.G. Schoenfeld, D. Goorvitch, C. Chackerian, H. Dothe, F. Mélen, M.C. Abrams, J.E.A. Selby, Updated line parameters for OH $X^2\Pi-X^2\Pi(v'', v')$ transitions, *J. Quant. Spectrosc. Radiat. Transfer* 59 (1998) 453–469.
- [37] P. Mezei, T. Cserfalvi, Charge densities in the electrolyte cathode atmospheric glow discharge (ELCAD), *Eur. Phys. J. Appl. Phys.* 40 (2007) 89–94.